

Superfluid density and superconducting gaps of RbFe_2As_2 as a function of hydrostatic pressure

Z. Shermadini,^{1,*} H. Luetkens,¹ A. Maisuradze,^{1,2} R. Khasanov,¹ Z. Bukowski,^{3,4} H.-H. Klauss,⁵ and A. Amato¹

¹*Laboratory for Muon Spin Spectroscopy, Paul Scherrer Institute, CH-5232 Villigen PSI, Switzerland*

²*Physik-Institut der Universität Zürich, Winterthurerstrasse 190, CH-8057 Zürich, Switzerland*

³*Laboratory for Solid State Physics, ETH Zürich, CH-8093 Zürich, Switzerland*

⁴*Institute of Low Temperature and Structure Research,*

Polish Academy of Sciences, 50-422 Wrocław, Poland

⁵*Institut für Festkörperphysik, TU Dresden, D-01069 Dresden, Germany*

The superfluid density and superconducting gaps of superconducting RbFe_2As_2 have been determined as a function of temperature, magnetic field and hydrostatic pressure by susceptibility and muon-spin spectroscopy (μSR) measurements. From the data, fundamental microscopic parameters of the superconducting state like the London penetration depth λ , the gap values Δ , the upper critical field B_{c2} , and the Ginzburg-Landau parameter κ have been obtained. In accordance with earlier measurements the ratio of the superfluid density $n_s \propto \lambda^{-2}$ to the superconducting transition temperature $T_c = 2.52(2)$ K at ambient pressure is found to be much larger in the strongly hole-overdoped RbFe_2As_2 than in high- T_c Fe-based and other unconventional superconductors. As a function of pressure T_c strongly decreases with a rate of $dT_c/dp = -1.32$ K GPa⁻¹, i.e. it is reduced by 52% at $p = 1$ GPa. The temperature dependence of n_s is best described by a two gap s -wave model with both superconducting gaps being decreased by hydrostatic pressure until smaller gap completely disappears at $p = 1$ GPa.

I. INTRODUCTION

The antiferromagnetic BaFe_2As_2 is a mother compound of the “122” family of the iron-based arsenide unconventional superconductors. It crystallizes in the tetragonal ThCr_2Si_2 crystal structure with the space group of $I4/mmm$.¹ High temperature superconductivity can be induced in this system either by isovalent substitution^{2–7}, chemical charge carrier doping^{8,9} or hydrostatic pressure^{10–14} highlighting the large flexibility of the recently discovered iron-based superconductors to tune its electronic properties in general. Highest superconducting transition temperatures are achieved by hole doping in $\text{Ba}_{1-x}\text{A}_x\text{Fe}_2\text{As}_2$ upon substituting Ba by $\text{A} = \text{K}$ ⁹ or Rb ^{15–17} with a gradual transition from the magnetically ordered ground state¹⁸ towards a superconducting state as a function of x . The optimal superconducting transition temperature up to $T_c \simeq 38$ K is reached for $x \simeq 0.4$ in both cases^{9,17}. Different hole and electron bands are crossing the Fermi level in case of the optimal doped system as revealed by angle-resolved photoemission spectroscopy.^{19–21} The topology of the Fermi surface is basically dominated by big hole bands around the Γ point and small electron bands at the M point presenting favorable nesting conditions possibly related to the magnetic instabilities. This favorable topology is also thought to lead to interband processes playing an important role for the superconducting state.²² Indication of multi-gap superconductivity in the hole-doped system $\text{Ba}_{1-x}\text{Rb}_x\text{Fe}_2\text{As}_2$ was confirmed by our recent μSR measurements¹⁷. Further hole doping reduces T_c down to 3.5 K and 2.6 K for $\text{A} = \text{K}$ and Rb ,²³ for $x = 1$ and shifts the electron bands to the unoccupied side.²⁴ Therefore, one expects an absence of nesting conditions and hence of magnetic order, as confirmed for example by

our μSR zero field (ZF) measurements.²⁵ Another consequence is a strong decrease of the interband processes which might be related to the collapse of T_c . Furthermore, it was found that the superfluid density for the end compound of the series, RbFe_2As_2 , is much larger than in other Fe-based and unconventional superconductors¹⁷. This might signal a more conventional nature of the superconducting ground state. A further microscopic characterization of this compound seems highly mandatory since it may, in comparison with the optimally doped compounds from the same series, provide valuable information on the origin of high- T_c superconductivity in Fe-based materials. Therefore, we extended our earlier μSR studies on RbFe_2As_2 by performing measurements under hydrostatic pressure. Due to its comparatively low upper critical field $B_{c2} = 2.6(1)$ T and its reduced $T_c = 2.52(2)$ K, this system allows to study a large section of the $B - T - p$ phase diagram. As exemplified by a number of recent studies, the μSR technique is very well suited to investigate iron-based superconductors (see, for example, Ref. 26) and to provide quantitative measures of several microscopic parameters of the superconducting ground state. Here we report the determination of T_c , the London penetration depth λ and hence the superfluid density $n_s \propto \lambda^{-2}$, the superconducting gap values Δ , the upper critical field B_{c2} , and the Ginzburg-Landau parameter κ as a function of hydrostatic pressure. From our study it follows that the superconducting state in RbFe_2As_2 is indeed conventional and that hydrostatic pressure pushes it even further to the classical regime. Therefore a comparison of the electronic properties of RbFe_2As_2 under pressure with optimally doped members of the same family may provide essential information on the origin of the high- T_c phenomena in Fe-based superconductors.

II. EXPERIMENTAL DETAILS

The polycrystalline sample of RbFe_2As_2 , used for the present experiment, was synthesized in a two steps procedure at the Laboratory for Solid State Physics of the ETH-Zürich.¹⁶ First, RbAs and Fe_2As were prepared from pure elements in evacuated and sealed silica tubes. Then, appropriate amounts of RbAs and Fe_2As were mixed, pressed into 8 mm diameter pellets and annealed at 650 °C for several days in evacuated and sealed silica ampoules. The quality has been tested by x-ray diffraction and confirmed by our previous μSR studies at ambient pressure²⁵ that the sample is free from the magnetic ordering. Then, these cylindrical shaped synthesized pellets with total height of 10 mm were loaded into the CuBe pressure cell using Daphne oil as a pressure transfer medium. AC susceptibility measurements were performed with a conventional lock-in amplifier at 0, 0.27, 0.46, 0.68 and 0.98 GPa pressures in a temperature interval of 1.4-10 K, using the same pressure cell as for μSR . Additional, magnetization data were obtained for pressures up to 5.4 GPa on a commercial *Quantum Design* 7 T Magnetic Property Measurement System XL SQUID Magnetometer using a home-made diamond anvil cell at temperatures between 1.8 K and 10 K. Small lead (Pb) probes were used for pressure determination utilizing the pressure dependence of $T_{c,\text{Pb}}$.²⁷

The μSR measurements under pressure were performed at the μE1 beamline of the Paul Scherrer Institute (Villigen, Switzerland), using the GPD instrument equipped with an Oxford sorption pumped ^3He cryostat at temperatures down to 0.27 K. The pressure cells used during the μSR measurement and experimental setup are described elsewhere.^{28,29} Data were collected at magnetic fields up to 0.25 T and for the three pressures 0.2, 0.6 and 1.0 GPa. Zero pressure data are taken from our early experiments.²⁵ High-energy muons with a momentum of 105 MeV c^{-1} were used in order to penetrate the pressure cell walls. The typical statistics for both forward and backward detectors were 7 millions. The fraction of the muons stopping in the sample was about 45% while the remaining fraction stops in the pressure cell. Three different transverse (TF) as well as zero field (ZF) μSR measurements were done for each pressure point. The temperature dependence of the superfluid density were analyzed with the fitting package *musrfit* developed by A. Suter and B. Wojek.³⁰

III. RESULTS AND DISCUSSION

Figure. 1 exhibits the AC susceptibility data for pressure up to 1.0 GPa together with the pressure dependence of T_c . At ambient pressure the superconducting transition temperature of RbFe_2As_2 is $T_c = 2.55(2)\text{K}$ and it decreases linearly upon increasing the pressure with a rather large value of $dT_c/dp = -1.32 \text{ K GPa}^{-1}$. A linear extrapolation of the data suggests that superconductivity

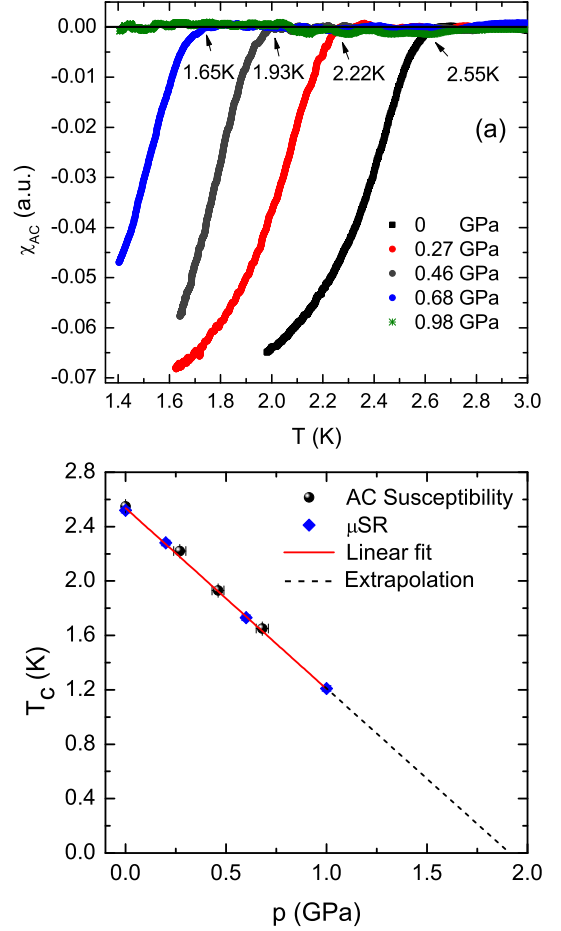


FIG. 1: (a) AC susceptibility measurements up to 1.0 GPa obtained with the same CuBe pressure cell as the one used for the μSR experiments. (b) Pressure dependence of T_c . The red solid line corresponds to a linear fit, and the dashed black line is an extrapolation up to 1.92 GPa.

could be completely suppressed by a pressure of approximately 2 GPa. In most superconductors, T_c is found to decrease under pressure, with some exceptions as in the cuprate oxides or some iron-based systems, which exhibit a remarkable increase.^{31,32} We note that a similarly large negative slope was found in another multi-gap superconductor MgB_2 where T_c decreases under pressure at a rate of $dT_c/dp \simeq -1.11 \text{ K GPa}^{-1}$ (see ref. 33,34).

The time evolution of the μSR signal is best described by the polarization function:²⁹

$$A_0 P(t) = A_s \exp\left[-\frac{(\sigma_s^2 + \sigma_n^2)}{2} t^2\right] \cos(\gamma_\mu B_{\text{int}} t + \varphi) + A_{\text{pc}} \exp\left[-\frac{\sigma_{\text{pc}}^2}{2} t^2\right] \int P(B_{\text{pc}}) \cos(\gamma_\mu B_{\text{pc}} t + \varphi) dB_{\text{pc}}, \quad (1)$$

where the first term corresponds to the signal arising from the sample with the corresponding parameters: A_s : initial asymmetry; σ_{sc} : second moment of the magnetic field distribution due to the flux line lattice (FLL) in

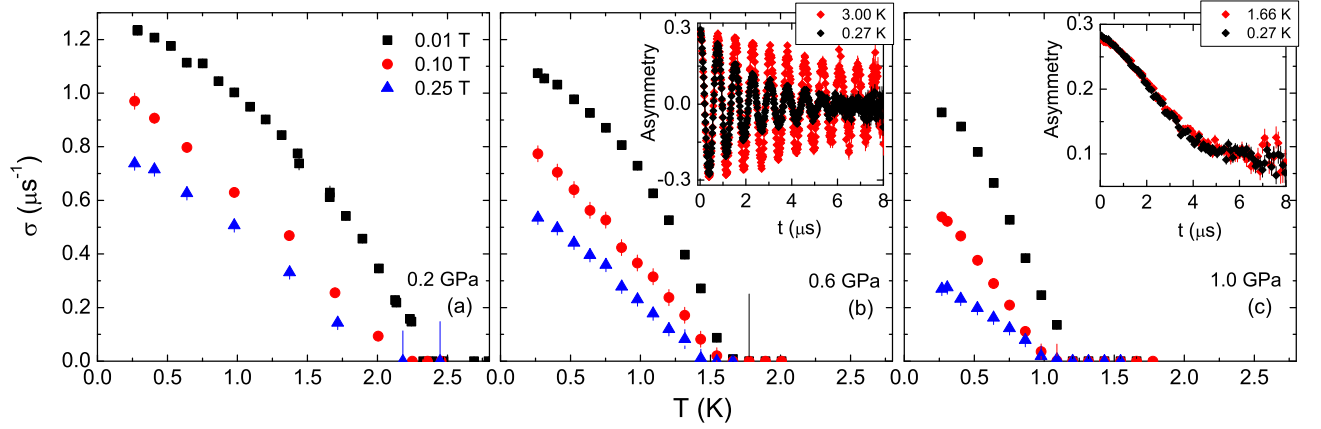


FIG. 2: Temperature dependence of $\sigma_s(T)$ obtained for RbFe_2As_2 at different pressures. For each pressure, measurements at different fields were performed. The insert on the panel (b) corresponds to TF, and on the panel (c) - ZF μSR time spectra above and below T_c at 1.0 GPa pressure.

the mixed state; σ_n : depolarization rate due to the nuclear moments; and B_{int} : internal magnetic field at the muon site. The second term on the right-hand side of Eq. 1 represents the pressure cell contribution. A_{pc} denotes the initial asymmetry; $\sigma_{\text{pc}} = 0.27 \mu\text{s}^{-1}$: field and temperature independent Gaussian relaxation rate of the CuBe pressure-cell material; and B_{pc} is magnetic field sensed by the muons stopped in the pressure cell. $\gamma_\mu = 135.5342 \times 2\pi \text{ MHz T}^{-1}$ is the muon gyromagnetic ratio and φ is the initial phase of the muon spin polarization. $P(B_{\text{pc}})$ is a distribution of magnetic fields sensed by the muons in the pressure cell which is calculated using Eq. (A4) of reference 29. Therefore the integral is invoked to describe the sum of the applied field and the field induced by the sample in a diamagnetic state.

For each pressure point zero-field (ZF) μSR measurements have been performed to check the magnetic properties of the system. No sign of magnetism neither static order nor slow magnetic fluctuations has been observed up to the highest pressure investigated in this study. This is illustrated by the ZF spectra at 1.0 GPa shown in the insert of Fig. 2 (c).

The superconducting properties were investigated by transverse field (TF) μSR measurements in the mixed state after field cooling which ensures the formation of a uniform FLL. Fitting Eq. (1) to the μSR time spectra, we obtain the temperature, magnetic field and pressure dependent parameters $\sigma_{\text{sc}}(T, B, p)$ [see Fig. 2(a,b,c)]. Using the numerical Ginzburg-Landau model developed by Brandt:³⁵

$$\sigma_s [\mu\text{s}^{-1}] = 4.83 \times 10^4 (1 - B_{\text{ext}}/B_{c2}) \times [1 + 1.21(1 - \sqrt{B_{\text{ext}}/B_{c2}})^3] \lambda^{-2} [\text{nm}] \quad (2)$$

one can fit the field dependent depolarization rate $\sigma_s(B_{\text{ext}})|_{T, p = \text{const.}}$ and evaluate two important parameters of the superconducting state, i.e. the London penetration depth λ and the upper critical field B_{c2} (see Fig. 3). This approach assumes that λ is field indepen-

dent, as it was confirmed by our previous zero pressure measurements.²⁵

As a second step, the temperature dependence of the superconducting carrier concentration $\rho_s = n_s(T)/n_s(0) = \lambda^{-2}(T)/\lambda^{-2}(0)$ is calculated from the inverse square of the penetration depth. It can be fitted using the local (London) approximation:³⁶

$$\rho_s = \frac{\lambda^{-2}(T)}{\lambda^{-2}(0)} = 1 - \frac{2}{k_B T} \int_{\Delta}^{\infty} f(\epsilon, T) [1 - f(\epsilon, T)] d\epsilon, \quad (3)$$

leaving $\lambda^{-2}(0)$ and $\Delta(0)$ as free parameters. Here $f(\epsilon, T) = [1 + \exp(\sqrt{\epsilon^2 + \Delta(T)^2}/k_B T)]^{-1}$ represents the Fermi function with the BCS spherical s -wave type of $\Delta(T)$ gap.³⁰ As evidenced by our previous study²⁵ a $s + s$ multigap model

$$\rho_s = \omega \rho_{s1} + (1 - \omega) \rho_{s2} \quad (4)$$

where ω is the relative weighting factor for the smaller gap, $\Delta_1(0)$, gives a satisfactory fitting result which is also supported by ARPES measurements where several disconnected Fermi-surface sheets are detected for another member of 122 iron arsenide family.¹⁹ The fitting results are shown in Fig. 3(b) and the pressure dependence of the parameters is reported on Fig. 4. It is found that the hydrostatic pressure only slightly reduces the superfluid density. Note that at 1.0 GPa, one does not require anymore the $s + s$ model and that a single s -wave gap scenario (i.e. $\omega \simeq 0$) is sufficient to describe the data. One may remark that upon increasing the hydrostatic pressure the positive curvature of $B_{c2}(T)$ near T_c gradually disappears and ends up with a usual BCS temperature dependence shape at 1.0 GPa [Fig. 3(a)], giving an additional indication of the disappearance of the smaller gap. Both gaps gradually decrease and at 1.0 GPa the small gap Δ_1 essentially disappeared [Fig. 4(a)]; corre-

spondingly, its weighting factor is falling from a maximum of $\omega = 0.36$ value to 0 [Fig. 4(b)]. The BCS ratios $2\Delta_1(0)/k_B T_c = 1.5(1)$ and $2\Delta_2(0)/k_B T_c = 4.5(1)$ are relatively independent on pressure up to 0.6 GPa followed by a gradual drop for the large gap value in the absence of the smaller gap. Upon increasing the hydrostatic pressure from 0 to 1.0 GPa, T_c is reduced by $\sim 52\%$, while the superfluid density $\rho \propto \lambda^{-2}$ is decreased by $\sim 18\%$, only. In other words, as shown in Fig. 4 (d), the superfluid density only weakly depends on the hydrostatic pressure in contrast to the strong dependence of T_c , typical for unconventional high- T_c superconductors where a proportionality of this two quantities is usually observed (at least in under- and optimally doped compounds). Using the pressure-dependent values of the penetration depths and upper critical field one can determine the characteristic ratio, known as the Ginzburg-Landau parameter, $\kappa = \lambda/\xi$, determined at our base temperature of 0.27 K.³⁶ ξ is a superconducting coherent length calculated from the relation $B_{c2} = \Phi_0/2\pi\xi^2$, where $\Phi_0 = 2.0678 \times 10^{-15}$ Wb is the magnetic flux quantum. A reduction of 50% of κ is determined at the highest available pressure of this experiment, pointing to a clear shift of the superconducting character of RbFe₂As₂ away from a strong type II superconductor towards low κ classical BCS superconductors. Interestingly, both T_c and κ linearly decrease with pressure and therefore we find the experimental correlation $\kappa \propto T_c$ (see Table I).

One way to visualize and to shed light onto the nature of the superconducting state has been presented by Uemura *et al.* in Refs. 37 and 38. According to the so-called ‘‘Uemura plot’’ the universal linear relation between T_c and $\sigma_s(T \rightarrow 0)$ has been found for high temperature superconductor cuprates. The critical temperature appears to be proportional to the inverse square of the London penetration depth $T_c \propto \rho_s \propto \lambda^{-2}$ for a large number of cuprate superconductors, but the proportionality constant is different for hole- and electron-doped superconductors.³⁹ A number of Fe-based superconductors appear to follow the Uemura relation (see Fig. 5). For comparison reason we include the data points of RbFe₂As₂ to the Uemura plot. As evidenced from Fig. 5, various families of unconventional superconductors including high- T_c Fe-based materials are characterized by small λ^{-2} values (superfluid density) compared to their T_c ; i.e. they exhibit a dilute superfluidity. In contrast, conventional phonon mediated superconductors like el-

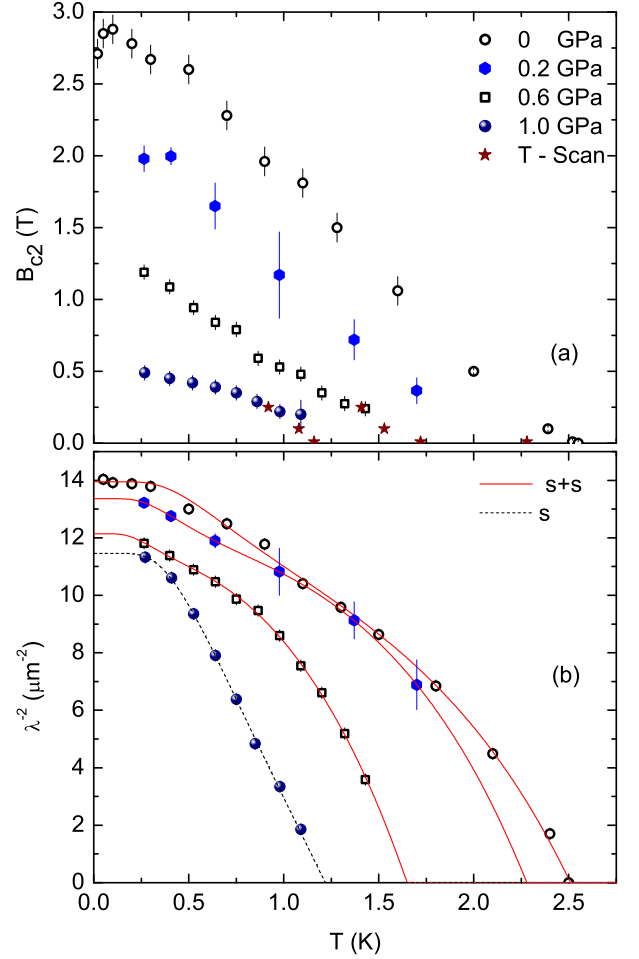


FIG. 3: (a) Temperature and pressure dependence of upper the critical field $B_{c2}(T)$. The stars corresponds to the values obtained by analyzing the temperature dependence of $\sigma_s(T)$. The other points are obtained by fitting Eq. 2 to the $\sigma_s(B_{\text{ext}})|_{T, p = \text{const.}}$ data. (b) Temperature and pressure dependence of $\lambda^{-2}(T)$. The solid lines correspond to a s+s-wave multi-gap fit model and the dashed one to a s-wave single-gap fit.

emental metals possess a dense superfluid, and exhibit low values of T_c . RbFe₂As₂ falls in between these two extreme cases. With increased hydrostatic pressure the critical temperature reduces rapidly, compared to superfluid density, and the relation of T_c to λ^{-2} moves closer to the one characteristic for conventional superconductors.

In the following, we discuss the different effects of chemical and hydrostatic pressure on the RbFe₂As₂ system. As mentioned above, the related compound KFe₂As₂ is also superconducting with an increased $T_c = 3.8$ K compared to $T_c = 2.6$ K in RbFe₂As₂. Due to the smaller ionic radius of K⁺ compared to Rb⁺ both the *a*- and *c*-axis parameters of KFe₂As₂ are reduced.^{9,15,18,23,40} In other words, in the up-to-now hypothetical series Rb_{1-y}K_yFe₂As₂ the increasing chemical pressure with increasing *y* should finally lead to the experimentally ob-

TABLE I: List of the pressure dependent parameters obtained from the analysis of $\lambda^{-2}(T)$.

<i>p</i> (GPa)	T_c (K)	$\Delta_1(0)$ (meV)	$\Delta_2(0)$ (meV)	$\frac{2\Delta_1(0)}{k_B T_c}$	$\frac{2\Delta_2(0)}{k_B T_c}$	κ	$\lambda(0)$ (nm)
0.00(0)	2.52(2)	0.15(2)	0.49(4)	1.5(2)	4.5(4)	24(1)	267(5)
0.20(1)	2.28(1)	0.11(3)	0.45(7)	1.1(3)	4.6(7)	21(1)	274(5)
0.60(1)	1.73(1)	0.08(4)	0.30(2)	1.1(6)	4.1(3)	17(1)	287(6)
1.00(2)	1.21(1)	0.00(0)	0.15(1)	0.0(0)	2.9(2)	12(1)	295(6)

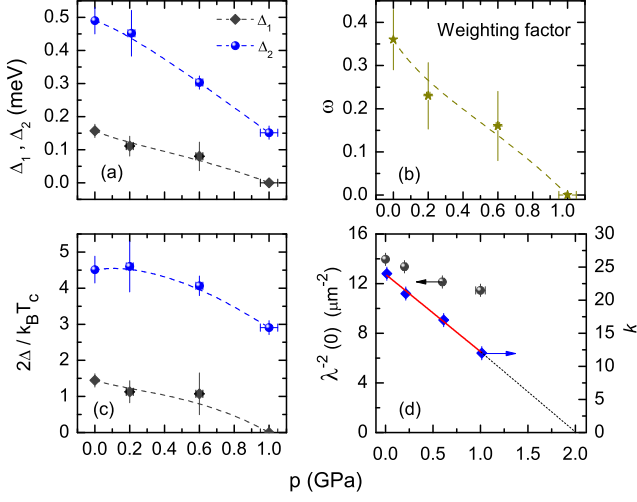


FIG. 4: Pressure dependence of: (a) the zero-temperature gap values $\Delta_1(0)$ and $\Delta_2(0)$, (b) the weight ω of the small gap, (c) the BCS ratios $2\Delta(0)/k_B T_c$ for both gaps, and (d) the inverse square of the penetration depth $\lambda^{-2}(0)$ and Ginzburg-Landau parameter κ . The lines are the guides to the eyes.

served increased T_c . In sharp contrast, our hydrostatic pressure experiments on RbFe₂As₂ show a strong reduction of T_c with increasing pressures. A possible way out of the apparent discrepancy could be a non-monotonic dependence of T_c on pressure with a reappearance of superconductivity at higher pressures as it was recently observed in another Fe-based superconductor.^{41,42} Therefore, we tested this hypothesis by performing further magnetization studies under high pressure using a diamond anvil cell. No superconducting transition was detected above 1.8 K up to our maximum pressure of 5.4 GPa. Based on these experimental facts, one has to conclude that external pressure is not equivalent to chemical pressure in this particular compound. This is probably related to the different effects of the two forms of pressure on the local atomic structure within the FeAs tetrahedra which is known to be one of the governing parameters determining T_c in Fe-based superconductors.⁴³

IV. SUMMARY AND CONCLUSION

To summarize, μ SR and magnetization measurements under hydrostatic pressures (0.2, 0.6 and 1.0 GPa) were carried out on the polycrystalline RbFe₂As₂ hole-overdoped iron-based superconductor. A negative pressure effect was observed on critical temperature with a rate of $dT_c/dp = -1.32$ K GPa⁻¹ in contrast to a positive effect expected for an equivalency of chemical and hydrostatic pressures. The zero temperature values of London penetration depth $\lambda(0)$, superconducting gaps $\Delta(0)$, upper critical field B_{c2} , and Ginzburg-Landau parameter $\kappa = \lambda/\xi$ have been evaluated from the experimental data.

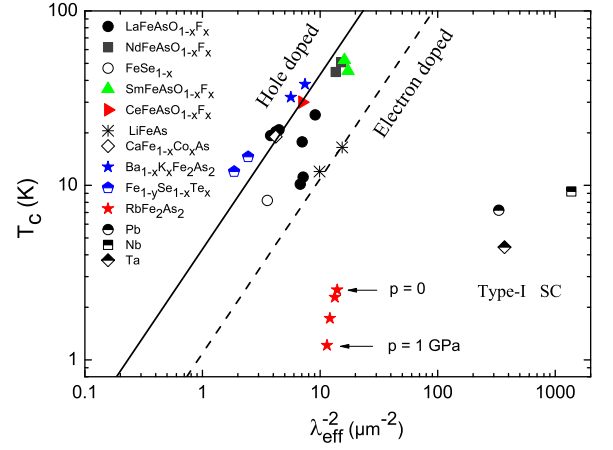


FIG. 5: Uemura plot for some Fe-based high temperature superconductors. The Uemura relation observed for underdoped cuprates is shown as a black dashed line for electron doping and as a solid line for hole doping [39]. The data are taken from the following references: LaFeAsO_{1-x}F_x - [44-47]. NdFeAs_{1-x}F_x - [44,48]. FeSe_{1-x} - [49,50]. SmFeAs_{1-x}F_x - [48,51]. CeFeAs_{1-x}F_x - [44]. LiFeAs - [52]. CaFe_{1-x}Co_xAs - [53]. Ba_{1-x}K_xFe₂As₂ - [20]. Fe_{1-y}Se_{1-x}Te_x - [54,55]. Pb, Nb and Ta - [56]. RbFe₂As₂ - obtained in this work and in [25].

The superfluid density was found to be weakly pressure dependent, while κ and T_c are linearly reduced by 50% by the application of pressures up to 1 GPa. Upon increasing the hydrostatic pressure, the system undergoes a transition from a $s + s$ -wave multi-gap superconducting state to a single s -wave gap state.

Here, one can highlight three main points in favor of tendency to the conventional BCS type of superconductors:

(i) Upon increasing the hydrostatic pressure RbFe₂As₂ compound exhibits a gradual transition from two gap to single gap state ending up with the BCS ratio of $2\Delta/k_B T_c = 2.9(2)$.

(ii) A Strong reduction of κ from 24 down to 12 is observed, getting closer to the conventional BCS superconductors, and in the limit of high pressures it extrapolates to value typical for the type I superconductors.

(iii) The Uemura classification scheme shows that with increased hydrostatic pressure the critical temperature reduces more rapidly than the superfluid density, and the relation of T_c to λ^{-2} moves closer to the region where low critical temperature and high superfluid density are characteristics for conventional superconductors.

Moreover, n_s is only diminished by 18% at $p = 1$ GPa indicating that the proportionality of n_s and T_c found for several families of under and optimally doped unconventional superconductors does not hold for RbFe₂As₂ either. On the other hand, these observations are rather typical for classical low temperature BCS superconductors.⁵⁷ In addition, the temperature dependence of n_s is best described by a two gap s -wave model

with both superconducting gaps being decreased by hydrostatic pressure until the smaller gap completely disappears at 1 GPa. Hence, the hydrostatic pressure appears to shift the nature of the ground state of the hole-overdoped RbFe_2As_2 system to an even more classical superconducting state. The superconducting ground state of the hole-overdoped RbFe_2As_2 system appears to be rather conventional. Since no superconducting transition was detected above 1.8 K up to 5.4 GPa pressure, one may conclude that external pressure is not equivalent to chemical pressure in this particular compound. The experimental and theoretical comparisons of the electronic properties of RbFe_2As_2 under pressure with optimally doped members of the same family should therefore pro-

vide new insight into the origin of the high- T_c phenomena in Fe-based superconductors.

V. ACKNOWLEDGMENTS

The μSR and magnetization experiments up to 1.0 GPa were performed at the Swiss Muon Source, Paul Scherrer Institute, Villigen, Switzerland. We acknowledge support by the Swiss National Science Foundation, the NCCR Materials with Novel Electronic Properties (MaNEP).

-
- * Corresponding author: zurab.sheradini@psi.ch
- ¹ M. Pfisterer and G. Nagorsen, *Z. Naturforsch.* **35** (1980).
 - ² W. Cao et al., *Europhysics Letters* **86**, 47002 (2009).
 - ³ K. Hashimoto, S. Kasahara, R. Katsumata, Y. Mizukami, M. Yamashita, H. Ikeda, T. Terashima, A. Carrington, Y. Matsuda, and T. Shibauchi, *Phys. Rev. Lett.* **108**, 047003 (2012).
 - ⁴ S. Jiang., H. Xing., G. Xuan., C. Wang., Z. Ren., C. Feng., J. Dai., Z. Xu., and G. Cao., *Journal of Physics: Condensed Matter* **21**, 382203 (2009).
 - ⁵ S. Kasahara, T. Shibauchi, K. Hashimoto, K. Ikada, S. Tonegawa, R. Okazaki, H. Shishido, H. Ikeda, H. Takeya, K. Hirata, et al., *Phys. Rev. B* **81**, 184519 (2010).
 - ⁶ Y. Qi, L. Wang, Z. Gao, D. Wang, X. Zhang, and Y. Ma, *Physica C* **469**, 1921 (2009).
 - ⁷ Z. R. Ye, Y. Zhang, F. Chen, M. Xu, Q. Q. Ge, J. Jiang, B. P. Xie, and D. L. Feng, *Phys. Rev. B* **86**, 035136 (2012).
 - ⁸ Y. Kamihara et al., *Am. Chem. Soc.* **130**, 32963297 (2008).
 - ⁹ M. Rotter, M. Tegel, and D. Johrendt, *Phys. Rev. Lett.* **101**, 107006 (2008).
 - ¹⁰ J. J. Hamlin, R. E. Baumbach, D. A. Zocco, T. A. Sayles, and M. B. Maple, *J. Phys.: Condens. Matter* **20**, 365220 (2008).
 - ¹¹ Y. Mizuguchi, F. Tomioka, S. Tsuda, T. Yamaguchi, and Y. Takano, *Appl. Phys. Lett.* **93**, 152505 (2008).
 - ¹² H. Okada, K. Igawa, H. Takahashi, Y. Kamihara, M. Hirano, H. Hosono, K. Matsubayashi, and Y. Uwatoko, *Journal of the Physical Society of Japan* **77**, 113712 (2008).
 - ¹³ H. Takahashi, K. Igawa, K. Arii, Y. Kamihara, M. Hirano, and H. Hosono, *Nature (London)* **453**, 376 (2008).
 - ¹⁴ A. D. Zocco, J. J. Hamlin, R. E. Baumbach, M. B. Maple, M. A. McGuire, A. S. Sefat, B. C. Sales, R. Jin, D. Mandrus, J. R. Jeffries, et al., *Physica C* **468**, 2229 (2008).
 - ¹⁵ Z. Bukowski, S. Weyeneth, R. Puzniak, P. Moll, S. Katrych, N. D. Zhigadlo, J. Karpinski, H. Keller, and B. Batlogg, *Phys. Rev. B* **79**, 104521 (2009).
 - ¹⁶ Z. Bukowski et al., *Phys. C* **470**, S328 (2010).
 - ¹⁷ Z. Guguchia, Z. Sheradini, A. Amato, A. Maisuradze, A. Shengelaya, Z. Bukowski, H. Luetkens, R. Khasanov, J. Karpinski, and H. Keller, *Phys. Rev. B* **84**, 094513 (2011).
 - ¹⁸ M. Rotter, M. Tegel, D. Johrendt, I. Schellenberg, W. Hermes, and R. Pöttgen, *Phys. Rev. B* **78**, 020503 (2008).
 - ¹⁹ D. V. Evtushinsky et al., *New J. Phys.* **11**, 055069 (2009).
 - ²⁰ R. Khasanov, D. V. Evtushinsky, A. Amato, H.-H. Klauss, H. Luetkens, C. Niedermayer, B. Büchner, G. L. Sun, C. T. Lin, J. T. Park, et al., *Phys. Rev. Lett.* **102**, 187005 (2009).
 - ²¹ V. B. Zabolotnyy et al., *Nature* **457**, 569 (2009).
 - ²² H. Ding et al., *J. Phys.: Condens. Matter* **23**, 135701 (2011).
 - ²³ K. Sasmal, B. Lv, B. Lorenz, A. M. Guloy, F. Chen, Y.-Y. Xue, and C.-W. Chu, *Phys. Rev. Lett.* **101**, 107007 (2008).
 - ²⁴ T. Sato, K. Nakayama, Y. Sekiba, P. Richard, Y.-M. Xu, S. Souma, T. Takahashi, G. F. Chen, J. L. Luo, N. L. Wang, et al., *Phys. Rev. Lett.* **103**, 047002 (2009).
 - ²⁵ Z. Sheradini, J. Kanter, C. Baines, M. Bendele, Z. Bukowski, R. Khasanov, H.-H. Klauss, H. Luetkens, H. Maeter, G. Pascua, et al., *Phys. Rev. B* **82**, 144527 (2010).
 - ²⁶ A. Amato et al., *Phys. C* **469**, 606 (2009).
 - ²⁷ A. Eiling and J. S. Schilling, *J. Phys. F: Met. Phys.* **11**, 623 (1981).
 - ²⁸ D. Andreica, PhD Thesis, IPP/ETH-Zurich (2001).
 - ²⁹ A. Maisuradze, A. Shengelaya, A. Amato, E. Pomjakushina, and H. Keller, *Phys. Rev. B* **84**, 184523 (2011).
 - ³⁰ A. Suter and B. M. Wojek, *Physics Procedia* **30**, 69 (2012).
 - ³¹ L. Gao, Y. Y. Xue, F. Chen, Q. Xiong, R. L. Meng, D. Ramirez, C. W. Chu, J. H. Eggert, and H. K. Mao, *Phys. Rev. B* **50**, 4260 (1994).
 - ³² M. K. Wu, J. R. Ashburn, C. J. Torng, P. H. Hor, R. L. Meng, L. Gao, Z. J. Huang, Y. Q. Wang, and C. W. Chu, *Phys. Rev. Lett.* **58**, 908 (1987).
 - ³³ S. Deemyad, T. Tomita, J. J. Hamlin, B. R. Beckett, J. S. Schilling, D. G. Hinks, J. D. Jorgensen, S. Lee, and S. Tajima, *Physica C* **385**, 105 (2003).
 - ³⁴ J. S. Schilling, Springer Verlag **Hamburg, March**, A Treatise on Theory and Applications, edited by J. R. Schrieffer (2006).
 - ³⁵ E. H. Brandt, *Phys. Rev. B* **68**, 054506 (2003).
 - ³⁶ M. Tinkham, *Introduction to Superconductivity* (McGraw-Hill Inc. New York., 1996).
 - ³⁷ Y. J. Uemura, L. P. Le, G. M. Luke, B. J. Sternlieb, W. D. Wu, J. H. Brewer, T. M. Riseman, C. L. Seaman, M. B. Maple, M. Ishikawa, et al., *Phys. Rev. Lett.* **66**, 2665 (1991).
 - ³⁸ Y. J. Uemura, G. M. Luke, B. J. Sternlieb, J. H. Brewer, J. F. Carolan, W. N. Hardy, R. Kadono, J. R. Kempton,

- R. F. Kiefl, S. R. Kreitzman, et al., Phys. Rev. Lett. **62**, 2317 (1989).
- ³⁹ A. Shengelaya, R. Khasanov, D. G. Eshchenko, D. Di Castro, I. M. Savić, M. S. Park, K. H. Kim, S.-I. Lee, K. A. Müller, and H. Keller, Phys. Rev. Lett. **94**, 127001 (2005).
- ⁴⁰ M. Rotter et al., Chem. Int. Ed. **47**, 7949 (2008).
- ⁴¹ J. Guo, X.-J. Chen, J. Dai, C. Zhang, J. Guo, X. Chen, Q. Wu, D. Gu, P. Gao, L. Yang, et al., Phys. Rev. Lett. **108**, 197001 (2012).
- ⁴² L. Sun et al., Nature **483**, 67 (2012).
- ⁴³ Y. Mizuguchi et al., Supercond. Sci. Technol. **23**, 054013 (2010).
- ⁴⁴ J. P. Carlo, Y. J. Uemura, T. Goko, G. J. MacDougall, J. A. Rodriguez, W. Yu, G. M. Luke, P. Dai, N. Shannon, S. Miyasaka, et al., Phys. Rev. Lett. **102**, 087001 (2009).
- ⁴⁵ H. Luetkens, H.-H. Klauss, R. Khasanov, A. Amato, R. Klingeler, I. Hellmann, N. Leps, A. Kondrat, C. Hess, A. Köhler, et al., Phys. Rev. Lett. **101**, 097009 (2008).
- ⁴⁶ H. Luetkens et al., Nature Materials **8**, 305 (2009).
- ⁴⁷ S. Takeshita et al., New J. Phys. **11**, 035006 (2009).
- ⁴⁸ R. Khasanov, H. Luetkens, A. Amato, H.-H. Klauss, Z.-A. Ren, J. Yang, W. Lu, and Z.-X. Zhao, Phys. Rev. B **78**, 092506 (2008).
- ⁴⁹ R. Khasanov, M. Bendele, A. Amato, K. Conder, H. Keller, H.-H. Klauss, H. Luetkens, and E. Pomjakushina, Phys. Rev. Lett. **104**, 087004 (2010).
- ⁵⁰ R. Khasanov, K. Conder, E. Pomjakushina, A. Amato, C. Baines, Z. Bukowski, J. Karpinski, S. Katrych, H.-H. Klauss, H. Luetkens, et al., Phys. Rev. B **78**, 220510 (2008).
- ⁵¹ A. J. Drew, F. L. Pratt, T. Lancaster, S. J. Blundell, P. J. Baker, R. H. Liu, G. Wu, X. H. Chen, I. Watanabe, V. K. Malik, et al., Phys. Rev. Lett. **101**, 097010 (2008).
- ⁵² F. L. Pratt, P. J. Baker, S. J. Blundell, T. Lancaster, H. J. Lewtas, P. Adamson, M. J. Pitcher, D. R. Parker, and S. J. Clarke, Phys. Rev. B **79**, 052508 (2009).
- ⁵³ S. Takeshita, R. Kadono, M. Hiraishi, M. Miyazaki, A. Koda, S. Matsuishi, and H. Hosono, Phys. Rev. Lett. **103**, 027002 (2009).
- ⁵⁴ M. Bendele, S. Weyeneth, R. Puzniak, A. Maisuradze, E. Pomjakushina, K. Conder, V. Pomjakushin, H. Luetkens, S. Katrych, A. Wisniewski, et al., Phys. Rev. B **81**, 224520 (2010).
- ⁵⁵ H. Kim, C. Martin, R. T. Gordon, M. A. Tanatar, J. Hu, B. Qian, Z. Q. Mao, R. Hu, C. Petrovic, N. Salovich, et al., Phys. Rev. B **81**, 180503 (2010).
- ⁵⁶ A. Suter, E. Morenzoni, N. Garifanov, R. Khasanov, E. Kirk, H. Luetkens, T. Prokscha, and M. Horisberger, Phys. Rev. B **72**, 024506 (2005).
- ⁵⁷ R. Khasanov, P. S. Häfliger, N. Shitsevalova, A. Dukhnenko, R. Brütsch, and H. Keller, Phys. Rev. Lett. **97**, 157002 (2006).